To link to this article : DOI:10.1016/j.ijmultiphaseflow.2015.07.004
URL : http://dx.doi.org/10.1016/j.ijmultiphaseflow.2015.07.004

Lattice Boltzmann model for predicting the deposition of inertial particles transported by a turbulent flow

Pascal Fede [a,b,*], Victor Sofonea [c], Richard Fournier [d,b], Stéphane Blanco [d,b], Olivier Simonin [a,b], Guillaume Lepoutère [a,b], Victor Ambruş [c]

[a] Université de Toulouse; INPT, UPS, Institut de Mécanique des Fluides de Toulouse, Allée Camille Soula, FR-31400 Toulouse, France
[b] CNRS, Fédération de Recherche FERMAT, FR-31400 Toulouse, France
[c] Center for Fundamental and Advanced Technical Research, Romanian Academy, Bd. Mihai Viteazul 24, RO-300223 Timisoara, Romania
[d] Université de Toulouse; INPT, UPS, LAPLACE, 118, route de Narbonne, FR-31062 Toulouse, France

Keywords:
Lattice Boltzmann
Kinetic approach
Particle-turbulence interaction
Deposition

A B S T R A C T

Deposition of inertial solid particles transported by turbulent flows is modelled in a framework of a statistical approach based on the particle velocity Probability Density Function (PDF). The particle-turbulence interaction term is closed in the kinetic equation by a model widely inspired from the famous BGK model of the kinetic theory of rarefied gases. A Gauss-Hermite Lattice Boltzmann model is used to solve the closed kinetic equation involving the turbulence effect. The Lattice Boltzmann model is used for the case of the deposition of inertial particles transported by a homogeneous isotropic turbulent flows. Even if the carrier phase is homogeneous and isotropic, the presence of the wall coupled with particle-turbulence interactions leads to inhomogeneous particle distribution and non-equilibrium particle fluctuating motion. Despite these complexities the predictions of the Lattice Boltzmann model are in very good accordance with random-walk simulations. More specifically the mean particle velocity, the r.m.s. particle velocity and the deposition rate are all well predicted by the proposed Lattice Boltzmann model.

Introduction

Solid inertial particles suspended in turbulent flows are involved in many practical applications such as coal combustion, particulate radioactive contamination, sediment transport or ripple motion, pollutant deposition, or drug inhalation by medicinal aerosols. In these applications, the deposition of the particles can be of great importance. From the modelling point of view, the particle deposition is challenging because the particle-turbulence interaction leads to several regimes. In a standard manner the particle-turbulence interaction is quantified with the Stokes number that is written in a turbulent channel flow as $\tau_p^* = \tau_p u^{*2}/\nu_f$, where τ_p is the particle relaxation time ($\tau_p = \rho_p d_p^2/18\rho_f \nu_f$) and ν_f/u^{*2} is a characteristic wall-turbulence time scale, defined on the basis of a boundary layer characteristic velocity u^*. In previous definitions, ρ_p is the particle density, d_p is the particle diameter and ν_f is the fluid viscosity. In boundary layer turbulence, we find three regimes (Friedlander and Johnstone, 1957):

- $\tau_p^* \ll 1$: a diffusion regime, where the particles behave like tracers.
- $\tau_p^* \gg 40$: an inertial regime, otherwise called ballistic regime, where the particles do not interact with the turbulence and achieve a free flight-like march down to the wall.
- $1 < \tau_p^* < 40$: a transitional regime corresponding to a partial interaction of the particles with the turbulence. It is a diffusion-impaction regime, appearing to be the most problematic regime to deal with.

These regimes are well described by Liu and Agarwal (1974) who made experiments in which they measured the deposition velocity of particles transported by the turbulent channel flow. To understand the mechanisms of the particle interaction with the near-wall turbulence, Direct Numerical Simulation coupled with Discrete Particle Simulation have been carried out (Kallio and Reeks, 1989; Marchioli et al., 2007). Besides these fundamental investigations, several modelling approaches have been developed,

* Corresponding author at: Université de Toulouse; INPT, UPS, Institut de Mécanique des Fluides de Toulouse, Allée Camille Soula, FR-31400 Toulouse, France.
E-mail address: pascal.fede@imft.fr (P. Fede).

http://dx.doi.org/10.1016/j.ijmultiphaseflow.2015.07.004

such as the ADE (Advection Diffusion Equation) models, from which the Euler/Euler, or the two-fluid models (Young and Leeming, 1997) showed a good capability only in the diffusion regime. In contrast, the approaches based on the Reynolds Averaged Navier Stokes (RANS) coupled with Lagrangian tracking of particles (Matida et al., 2000) were inaccurate for predicting the deposition rate and the near-wall region dynamics.

A way to model the behaviour of the inertial particles transported by a turbulent flow is to use a statistical description of the particle phase by a probability density function (PDF) of the particle velocity. In 2009, Aguinaga et al. (2009) proposed an original approach called SAB (for Simonin, Aguinaga and Borée) based on a kinetic equation where the interaction of the particle with the turbulence is closed by considering a return-to-equilibrium (BGK like) term. As shown by Aguinaga et al. (2009), the solution of this kinetic equation with pure deposition boundary condition can be tricky, even in the case where the turbulence is homogeneous and isotropic. Indeed, when considering the case of particles transported by a turbulent channel flow, Aguinaga et al. (2009) obtained good results for the impaction regime, while for the intermediate regime numerical problems appeared. More recently Van Dijk and Swailes (2012) proposed a novel methodology for the numerical treatment of multi-dimensional PDF models describing the particle transport in turbulent boundary layers. Diounou et al. (2011) proposed a very simple Lattice Boltzmann Model (LBM) approach to solve the SAB kinetic equation, which is more efficient and robust. In the present paper, a Gauss-Hermite Lattice Boltzmann Method (GHLBM) is proposed for solving directly the kinetic equation of the SAB model.

It must be emphasised the strong originality of the approach developed here. Indeed, solving the LBM evolution equation provides an alternative to solve the Navier–Stokes equations for single-fluid dynamics (Succi, 2001; Aidun and Clausen, 2010). The LBM was already used to investigate particle-laden flows, but only in order to compute the evolution of the interstitial fluid carrying the particles (Cate et al., 2004; Derksen and Sundaresan, 2007). In the present paper, the LBM approach is used to solve the PDF evolution kinetic equation that describes the dynamical behaviour of a cloud composed of solid particles.

The present study is a part of a more general work dedicated to Eulerian modelling of particle-laden turbulent flows showing complex interactions with walls, such as deposition or resuspension, but also non-elastic and/or frictional bouncing on rough wall. The derivation of boundary conditions in the frame of the Eulerian moment approach accounting for such complex particle–wall interaction mechanisms is a daunting task, in particular as a result of the non-equilibrium state of the particle velocity distribution in the near-wall region. To overcome the challenges, the final practical objective is to develop an hybrid method where the moment approach is used far from the wall and coupled with a full resolution method of the PDF kinetic equation towards the wall. The PDF resolution method could be a Lagrangian stochastic method, as proposed by Pialat et al. (2007b), or a LBM approach, as developed in the present paper, with the goal to simplify the coupling process with the moment approach used in the main flow.

The paper is organised as follows. First, the statistical approach describing the behaviour of solid particles interacting with a turbulent fluid flow is briefly introduced and the SAB model proposed by Aguinaga et al. (2009) is presented. The third section introduces the Lattice Boltzmann scheme. A focus is made on the numerical treatment of the term representing the forces acting on the particles. The role of the quadrature and of the Hermite expansion is illustrated by considering an academic problem, namely the homogeneous relaxation towards equilibrium. The LBM results for the deposition of inertial particles transported by a homogeneous isotropic turbulence are shown in the fourth section.

Statistical model

The statistical description of the dispersed phase, composed of solid particles or droplets transported by a turbulent fluid flow relies on the analogy with the thermal motion of molecules as described by the kinetic theory of rarefied gases. In the standard kinetic approach, the dispersed phase is described by the particle Probability Density Function $f_p(\mathbf{x}, t; \mathbf{c}_p)$ defined such that $f_p(\mathbf{x}, t; \mathbf{c}_p) d\mathbf{c}_p d\mathbf{x}$ is the mean probable number of particles at the time t with the centre of mass located in the volume $[\mathbf{x}, \mathbf{x} + d\mathbf{x}]$, and the translation velocity, $\mathbf{u}_p$, within $[\mathbf{c}_p, \mathbf{c}_p + d\mathbf{c}_p]$. From the PDF the density number of particles writes

$$n_p = \int f_p d\mathbf{c}_p, \tag{1}$$

the mean particle velocity,

$$U_{p,i} = \frac{1}{n_p} \int c_{p,i} f_p d\mathbf{c}_p, \tag{2}$$

and the particle kinetic stress,

$$\langle u'_{p,i} u'_{p,j} \rangle = \frac{1}{n_p} \int [c_{p,i} - U_{p,i}] \times [c_{p,j} - U_{p,j}] f_p d\mathbf{c}_p. \tag{3}$$

The single particle velocity PDF obeys the following Boltzmann-like kinetic equation:

$$\frac{\partial f_p}{\partial t} + \frac{\partial}{\partial x_i}[c_{p,i} f_p] + \frac{\partial}{\partial c_{p,i}}\left[\left\langle \frac{du_{p,i}}{dt} | \mathbf{c}_p \right\rangle f_p\right] = \left(\frac{\partial f_p}{\partial t}\right)_{col} \tag{4}$$

where $\langle . | \mathbf{c}_p \rangle$ is the ensemble average conditioned by the particle velocity. The third term on the left-hand-side of Eq. (4) represents the forces acting on the particles, enclosing the turbulent particle–fluid coupling. The term on the right-hand-side of Eq. (4) is the modification of the PDF by the inter-particle collisions. In the present study the particulate phase is very dilute such that this term will no longer be considered. For spherical particles transported by a turbulent flow, several forces are acting on the particles: the drag force, the lift force or the added mass force, as in (Gatignol, 1983; Maxey and Riley, 1983). However, assuming a large particle-to-fluid density ratio, the forces can be reduced to the gravity and drag forces. Then the particle acceleration reads

$$\frac{d\mathbf{u}_p}{dt} = -\frac{\mathbf{u}_p - \mathbf{u}_{f@p}}{\tau_p} + \mathbf{g} \tag{5}$$

where $\mathbf{u}_{f@p}$ is the fluid velocity at the particle position, $\mathbf{g}$ is the gravity and τ_p is the particle relaxation time. So using Eq. (5) in the third term of Eq. (4) and neglecting gravity, the Boltzmann equation becomes

$$\frac{\partial f_p}{\partial t} + \frac{\partial}{\partial x_i}[c_{p,i} f_p] + \frac{\partial}{\partial c_{p,i}}\left[-\frac{1}{\tau_p}(c_{p,i} - \langle u_{f@p,i} | \mathbf{c}_p \rangle) f_p\right] = 0. \tag{6}$$

As the paper is dedicated to the modelling of the particle-turbulence interaction in the wall boundary layer flow, we may assume, without loss of generality that $\partial/\partial y \approx \partial/\partial z \approx 0$. Then, considering τ_p as a given value independent of the instantaneous particle velocity (such as in Stokes's drag law), the kinetic equation governing the wall-normal particle velocity PDF is obtained by integration of Eq. (4) on the velocity components in y- and z-directions and is written

$$\frac{\partial f_p}{\partial t} + \frac{\partial}{\partial x}[c_p f_p] + \frac{\partial}{\partial c_p}\left[-\frac{1}{\tau_p}(c_p - \langle u_{f@p} | c_p \rangle) f_p\right] = 0 \tag{7}$$

where c_p is the particle velocity component expected in the x-direction normal to the wall.

The modelling of the particle-turbulence coupling term received much attention (Derevich and Zaichik, 1988; Zaichik et al., 1997; Reeks, 1992; Reeks, 1993; Simonin, 2000).

Aguinaga et al. (2009) proposed an approach inspired from the BGK model. The fluid-particle interaction term is separated in two contributions: first, the fluid-particle interaction through the mean gas and particle velocities; second, the coupling of the particle fluctuating motion with the fluid turbulence. The last contribution is modelled as a return-to-equilibrium term in a similar manner to the effect of the inter-particle interactions in the BGK model (Bhatnagar et al., 1954). As in the standard BGK model, the return-to-equilibrium term needs an "equilibrium" PDF, f^*, and a given time-scale, τ^*. Then Aguinaga et al. (2009) proposed to write the fluid-particle interaction terms of the kinetic equation as

$$\frac{\partial}{\partial c_p}\left[-\frac{1}{\tau_p}(c_p - \langle u_{f@p}|c_p\rangle)f_p\right] = -\left[\frac{U_p - U_{f@p}}{\tau_p}\right]\frac{\partial f_p}{\partial c_p} + \frac{\lambda}{\tau^*}\left[f_p - f^*\right]. \quad (8)$$

In Eq. (8) the equilibrium PDF, f^*, is chosen in order to model particles in equilibrium with the gas turbulence according to the Tchen & Hinze theory (Tchen, 1947; Hinze, 1972):

$$\left\langle u'_p u'_p\right\rangle = \left\langle u'_{f@p} u'_p\right\rangle = \left\langle u'_{f@p} u'_{f@p}\right\rangle \frac{1}{1+St} \quad (9)$$

with the Stokes number $St = \tau_p/\tau^t_{f@p}$, where $\tau^t_{f@p}$ represents the fluid Lagrangian integral time scale measured along the particle trajectories, which is proportional to the turbulent dissipation time scale $\tau^t_f = k/\epsilon$ (Simonin et al., 1993). But, in the present study, the LBM predictions are compared with stochastic simulation results from Nagy and Swailes (1996) with a given value of $\tau^t_{f@p}$. In such a framework, the equilibrium PDF is a Gaussian distribution (Laviéville et al., 1995)

$$f^*(x,t;c_p) = \frac{n_p}{\left(2\pi\left\langle u'_{f@p}u'_p\right\rangle\right)^{1/2}} \exp\left[-\frac{(c_p - U_p)^2}{2\left\langle u'_{f@p}u'_p\right\rangle}\right]. \quad (10)$$

The relaxation time-scale, τ^*, and the parameter λ in Eq. (8) are chosen to ensure exact fluid-particle interaction terms in the moment equations of n_p, U_p, and of the particle kinetic energy. This process leads to $\lambda = 2$ and $\tau^* = \tau_p$.

For the mean contribution, the mean fluid velocity seen by the particles, $U_{f@p}$, has been introduced. Such a mean velocity has two contributions: (i) the mean fluid velocity U_f and (ii) a drift velocity V_d representing the correlation between the local instantaneous particle distribution and the turbulent fluid velocity. Then the mean fluid velocity seen by the particles is written as $U_{f@p} = U_f + V_d$ and, following Simonin et al. (1993), the drift velocity in homogeneous turbulence reads

$$V_d = -\tau^t_{f@p}\left\langle u'_f u'_p\right\rangle \frac{1}{n_p}\frac{\partial n_p}{\partial x}. \quad (11)$$

Finally the Boltzmann-like transport Eq. (6) with the SAB model for the fluid-particle interaction becomes

$$\frac{\partial f_p}{\partial t} + c_p\frac{\partial f_p}{\partial x} + \left[\frac{U_p - (U_f + V_d)}{\tau_p}\right]\frac{\partial f_p}{\partial c_p} + \frac{2}{\tau_p}\left[f_p - f^*\right] = 0. \quad (12)$$

Aguinaga et al. (2009) solved this equation with a finite-difference scheme based on a non-uniform mesh. For particles with large particle relaxation times, the results were very good. However, the method was unstable for moderate and small Stokes number. In the next section, a Lattice Boltzmann scheme is proposed to solve Eq. (12).

Lattice Boltzmann model

Background

The lattice Boltzmann simulation of far out-of-equilibrium gas flows has received a solid theoretical attention with the work of Chen and co-workers (Zhang et al., 2006; Shan et al., 2006; Chen et al., 2007; Colosqui et al., 2009; Colosqui, 2010). These developments find their origin in intensive efforts made since 1997 towards the rigorous proof that numerous of the most established Lattice Boltzmann algorithms could be interpreted as numerical solutions of the Boltzmann equation itself (He and Luo, 1997; Abe, 1997; Shan and He, 1998; Piaud et al., 2005). A clear synthesis is that of Shan et al. (2006), leading to the proposition of a systematic approach based on a Hermite expansion of the Boltzmann equation similar to that of Grad in 1949 (Grad, 1949; Grad, 1952). In this approach, the starting point is the Boltzmann-BGK equation in which both the force term and the equilibrium distribution in the collision term are replaced by Hermite expansions. Then it is shown that truncating these Hermite expansions at a given order is equivalent to a strict satisfaction of all the moment equations in Grad's theory up to a fixed order, and that using a Gauss-Hermite quadrature in the Lattice Boltzmann velocity integration scheme maintains this strict satisfaction. Increasing the truncation order allows therefore to go as far as required into the field of far out-of-equilibrium phenomena.

Such an approach looks very much meaningful in the present context. The SAB model is indeed based on a transport equation very close to the Boltzmann-BGK equation and the problems of interest correspond to far out-of-equilibrium conditions under which a close description of the distribution function in phase space is required that cannot be easily reduced to the description of only the first three moments in geometrical space. Strong deviations from equilibrium have essentially two possible sources: the boundary conditions and the spatial variations of turbulent agitation. The analysis reported in the present text are restricted to homogeneous turbulence. The studied out-of-equilibrium conditions are directly related to the boundary conditions, essentially the fact that particle deposition at the wall is translated into a null value of the distribution function in the whole inward hemisphere. Thus, the distribution function at the wall is therefore very far from a Maxwellian distribution. The present question is therefore closely related to the treatment of boundary condition effects on the Boltzmann-BGK equation in rarefied gas flows. If we take this starting point when considering the lattice Boltzmann method for simulation of the SAB model, then the following differences must be pointed out. First of all, the variance of the Maxwellian distribution f^* is not equal to the variance of the local particle velocity distribution. As this variance (the local temperature) plays an essential part in the way the set of discrete velocities is chosen, the SAB model opens new specific questions. In particular, when adapting the available techniques, which of the two available local temperatures should be chosen, the particle "temperature" or the turbulence "temperature"? Another point is that the forces must be represented very accurately as they play an essential part in the considered particle-turbulence interaction physics, which is not the case in most of the reported implementations of Shan's proposition. From this point of view, a parallel can be made with the three-dimensional modelling of liquid–gas phase transition, which is today a very active area of research that will require the lattice Boltzmann methods to go through a very detailed further consideration of force terms in Boltzmann-like equations. Finally, the above mentioned fact that the variance of the Maxwellian distribution f^* is not equal to the variance of the local particle velocity has a positive consequence: the relaxation term of the SAB model is not energy conservative (energy is exchanged with turbulence) and we can assume that the addressed numerical problem will be less constrained, in terms of conservation principles, than those addressed for Boltzmann-BGK applications in rarefied gas flows.

Gauss-Hermite Lattice Boltzmann models in one dimension

In order to solve one-dimensional ($1D$) transport problems like the one defined by Eq. (12), which involves a relaxation process towards an equilibrium distribution function (Maxwellian) f^*, one can apply the general procedure described in Shan et al. (2006, 2014). According to this procedure, one introduces a $1D$ family of Gauss-Hermite Lattice Boltzmann models, denoted as GHLBM($N;Q$), where N is the order of the model and $Q \geqslant N+1$ is the quadrature order, i.e., the number of the vectors in the velocity set. The approximation of a PDF by using an expansion with respect to a family of orthogonal polynomials, followed by a quadrature method, is a quite standard technique used in LB models (Shan and He, 1998; Shan et al., 2006; Xiu and Karniadakis, 2002; Cho et al., 2014; Shizgal, 2015). Such a $1D$ Lattice Boltzmann (LB) model is said to be of order N (Shan et al., 2006; Piaud et al., 2014; Ambruş and Sofonea, 2012) if all the moments

$$\mathcal{M}^{eq,(s)}(x,t) = \int_{-\infty}^{+\infty} f_p^{eq} c_p^s dc_p, \qquad 0 \leqslant s \leqslant N \tag{13}$$

of the dimensionless equilibrium distribution function f^{eq} are exactly recovered for $U_p = 0$ and $T_p = 1$. This does not mean that the temporal evolution of the first N moments of the dimensionless distribution function f_p are recovered. Generally speaking, the number of the distribution function moments that are accurately predicted depends on the temporal and spatial Knudsen numbers, and even on the types of the considered initial and boundary conditions. But this is still clearly the objective of lattice - Boltzmann algorithms: accurately evaluating the moments of f_p up to a given order M, even at the expense of poorly evaluating the distribution function itself (which seems in contradiction with the kinetic nature of these algorithms). How this could be conceived as a meaningful objective is the result of a close combination of Hermite expansions (the same starting point as Grad) and Gauss-Hermite quadratures.

Expanding f_p in Hermite polynomials $\mathcal{H}^{(n)}(c_p)$, i.e., writing (Shan et al., 2006)

$$f_p \equiv f_p(x,t;c_p) = \omega(c_p)\sum_{n=0}^{\infty}\frac{1}{n!}a_n(x,t)\mathcal{H}_n(c_p) \tag{14}$$

with $\omega(c_p) = (1/\sqrt{2\pi})\exp\left[-c_p^2/2\right]$ and

$$a_n \equiv a_n(x,t) = \int f_p(x,t;c_p)\mathcal{H}_n(c_p)dc_p \tag{15}$$

allows one to define the truncated version of this expansion

$$f_p \simeq f_p^{(N)} \equiv f_p^{(N)}(x,t;c_p) = \omega(c_p)\sum_{n=0}^{N}\frac{1}{n!}a_n(x,t)\mathcal{H}_n(c_p) \tag{16}$$

that has exactly the same moments as f_p up to order N.

Using Gauss-Hermite quadratures of order $Q \geqslant N+1$ to compute the first N moments of $f_p^{(N)}$ would ensure that this computation is exact. This is because $f_p^{(N)}$ has, by construction, a Hermitian shape of order N,[1] and the Gauss-Hermite quadratures are precisely designed to evaluate the moments of such functions. So, if one manages to define and deal with the temporal evolution of $f_p^{(N)}$, then one only needs to evaluate it at the quadrature points $c_{p,k}$ $(k = 1,\ldots,Q)$. Thus, only Q values of $f_p^{(N)}$ are sufficient to get the exact values of the first N moments of $f_p^{(N)}$, that are identical to those of f_p:

$$\mathcal{M}^{(s)} \equiv \int_{-\infty}^{+\infty} f_p c_p^{(s)} dc_p = \mathcal{M}^{(N,s)} \equiv \int_{-\infty}^{+\infty} f_p^{(N)} c_p^{(s)} dc_p \tag{17}$$

for $0 \leqslant s \leqslant N$ and

$$\mathcal{M}^{(N,s)} = \sum_{k=1}^{Q}\frac{w_k}{\omega(c_{p,k})} f_{p,k}^{(N;Q)} c_{p,k}^s \tag{18}$$

for $Q \geqslant N+1$, with

$$f_{p,k}^{(N;Q)} \equiv f_{p,k}^{(N;Q)}(x,t) = f_p^{(N)}(x,t;c_{p,k}) \tag{19}$$

where w_k are the quadrature weights (Shan et al., 2006).

In practice, this ideal objective is never reached in an exact manner (except in academic cases such as the one that we develop in the following section for didactic purposes). Following Shan's approach (Shan et al., 2006), we start by replacing the true $f_p^{(N)}$ by another distribution function, $\tilde{f}_p \equiv \tilde{f}_p(x,t;c_p)$, that evolves according to the following transport equation ($\partial_t \equiv \partial/\partial t$ $\partial_x \equiv \partial/\partial x$), designed to recover a spatio-temporal evolution as close as possible to that of $f_p^{(N)}$:

$$\partial_t\tilde{f}_p + c_p\partial_x\tilde{f}_p - \mathbf{A}\omega(c_p)\sum_{n=0}^{N-1}\frac{1}{n!}\tilde{a}_n(x,t)\mathcal{H}_{n+1}(c_p) + \frac{2}{\tau_p}\left[\tilde{f}_p - f^{*(N)}\right] = 0 \tag{20}$$

with

$$\mathbf{A} = \left[\frac{U_p - (U_f + V_d)}{\tau_p}\right] \tag{21}$$

$$\tilde{a}_n = \int \tilde{f}(x,t;c_p)\mathcal{H}_n(c_p)dc_p \tag{22}$$

and

$$f^{*(N)} = \omega(c_p)\sum_{n=0}^{N}\frac{1}{n!}a_n^*(x,t)\mathcal{H}_n(c_p) \tag{23}$$

$$a_n^* = \int f^*(x,t;c_p)\mathcal{H}_n(c_p)dc_p \tag{24}$$

The transformed problem defined by Eq. (20) is obtained by projecting each term of the original equation into the space of Hermitian polynomials and truncating at order N. In fact, this is exactly true for all terms, except the transport term $c_p\partial_x\tilde{f}_p$ that cannot be justified using a strict truncation of $c_p\partial_x f_p$ at order N. Indeed, noting $(.)^{(N)}$ the hermitian projection truncated at order N, it can be easily checked that $\left(c_p\partial_x f_p\right)^{(N)} \neq c_p\partial_x f_p^{(N)}$. We will discuss this difference in Section 'The advection term', but in the following section we start by addressing simple homogeneous examples in which the advection term is null, ensuring that $\tilde{f}_p \equiv f_p^{(N)}$. Fig. 1 summarises the steps leading to a discrete problem in $\tilde{f}_p$ starting from the initial continuous f_p problem.

Homogeneous relaxation towards a Gaussian distribution

Let us consider the kinetic equation without the advection and force terms:

$$\partial_t f_p = -\frac{1}{\tau_p}\left(f_p - f^*\right). \tag{25}$$

[1] We refer to a *Hermitian shape of order N* each time a function of c_p is expressed as $\omega(c_p)$ times a weighted sum of the first N Hermite polynomials.

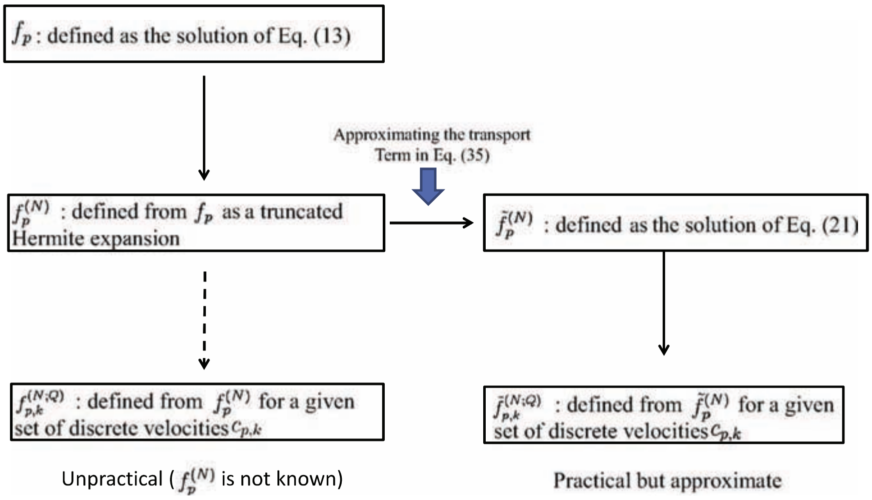

Fig. 1. Steps to transform the initial continuous problem into the practical problem that is solved.

This equation describes the homogeneous relaxation of the distribution function $f_p(c_p, t)$,

$$f_p(c_p, t) = f_0 e^{-t/\tau_p} + f^*(1 - e^{-t/\tau_p}) \tag{26}$$

where $f_0 \equiv f_p(c_p, t = 0)$. This allows us to easily integrate Eq. (26) to get the evolution equations of the moment of order M of f_p

$$\begin{aligned}\mathcal{M}^{(M)}(t) &= \int_{-\infty}^{+\infty} f_p(c_p, t) c_p^M dc_p \\ &= e^{-t/\tau_p} \int_{-\infty}^{+\infty} f_0 c_p^M dc_p + (1 - e^{-t/\tau_p}) \int_{-\infty}^{+\infty} f^* c_p^M dc_p \\ &= \mathcal{M}_0^{(M)} e^{-t/\tau_p} + \mathcal{M}^{*,(M)}(1 - e^{-t/\tau_p})\end{aligned} \tag{27}$$

For convenience, we will consider the case where both f_0 and f^* are Maxwellians:

$$f_0 = \frac{n_p}{\sqrt{2\pi T_{p,0}}} \exp\left[-\frac{(c_p - U_{p,0})^2}{2T_{p,0}}\right] \tag{28a}$$

$$f^* = \frac{n_p}{\sqrt{2\pi T_{p,*}}} \exp\left[-\frac{(c_p - U_{p,*})^2}{2T_{p,*}}\right] \tag{28b}$$

where $n_p, U_{p,0}, U_{p,*}, T_{p,0}$ and $T_{p,*}$ are constant quantities. So, the fluid starts in the Maxwellian state of velocity $U_{p,0}$ and temperature $T_{p,0}$ and relaxes toward the Maxwellian state of average velocity $U_{p,*}$ and temperature $T_{p,*}$ (see Fig. 2). Solving Eq. (25) using the Gauss-Hermite model GHLBM(N; Q) leads to the following evaluation of $\mathcal{M}^{(M)}$

$$\mathcal{M}_{N;Q}^{(M)}(t) = \sum_{k=1}^{Q} \tilde{f}_{p,k}^{(N;Q)}(t) c_{p,k}^M \tag{29}$$

with

$$\tilde{f}_{p,k}^{(N;Q)} \equiv \tilde{f}_{p,k}^{(N;Q)}(x, t) = \tilde{f}_p^{(N)}(x, t; c_{p,k}). \tag{30}$$

This solution can then be compared to Eq. (27) using the analytically known moments of the Maxwellian. The model GHLBM(N; Q) is expected to recover all the moments up to order $M = N$. Fig. 3 shows the evolution of all the moments up to order $M = 8$, as recovered using the models GHLBM(N; $Q = N + 1$), for $n_p = 1.0, U_{p,0} = -2.0, T_{p,0} = 1.0, U_{p,*} = 1.0$ and $T_{p,*} = 2.0$. For each N, we used only the minimum value of Q since the GHLBM(N; Q) models ensure all the moments of f_p up to order N for any $Q \geqslant N + 1$. For a given value of M, one can see that only the GHLBM models of order $N \geqslant M$ allow one to get the correct evolution of the moment $\mathcal{M}^{(M)}$ of the distribution function f_p subjected to the homogeneous relaxation process, Eq. (25). But then, above $N = M$ in this simple case, the moments are *strictly* exact, which will not be the case as soon as space gradients are present, inducing transport effects.

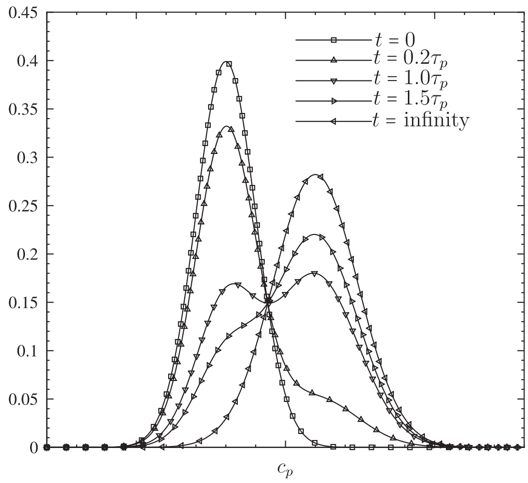

Fig. 2. Time-evolution of the distribution function $f_p(c_p, t)$ given by Eq. (26).

It is worth emphasising that the moments are exactly recovered, despite the fact that $\tilde{f}_{p,k}^{(Q;N)} \neq f_p(c_{p,k}, t)$: the computed values of the distribution function at the quadrature points do not match the true distribution. As shown by Fig. 4, they match its Hermite transform $f_p^{(N)}$:

$$\tilde{f}_{p,k}^{(N;Q)} = \tilde{f}_p(c_{p,k}, t) \quad \text{and} \quad \tilde{f}_p = f_p^{(N)} \tag{31}$$

This means for instance that $\tilde{f}_{p,k}^{(N;Q)}$ can take negative values in such an extreme case as that of Fig. 4. The initial and final distributions are so distinct ($T_{p,0} = 1, U_{p,0} = -2$ versus $T_{p,*} = 2, U_{p,*} = 1$) that the reference values T_{ref} and U_{ref}, used to render the problem dimensionless, cannot be chosen in an adequate manner so that the

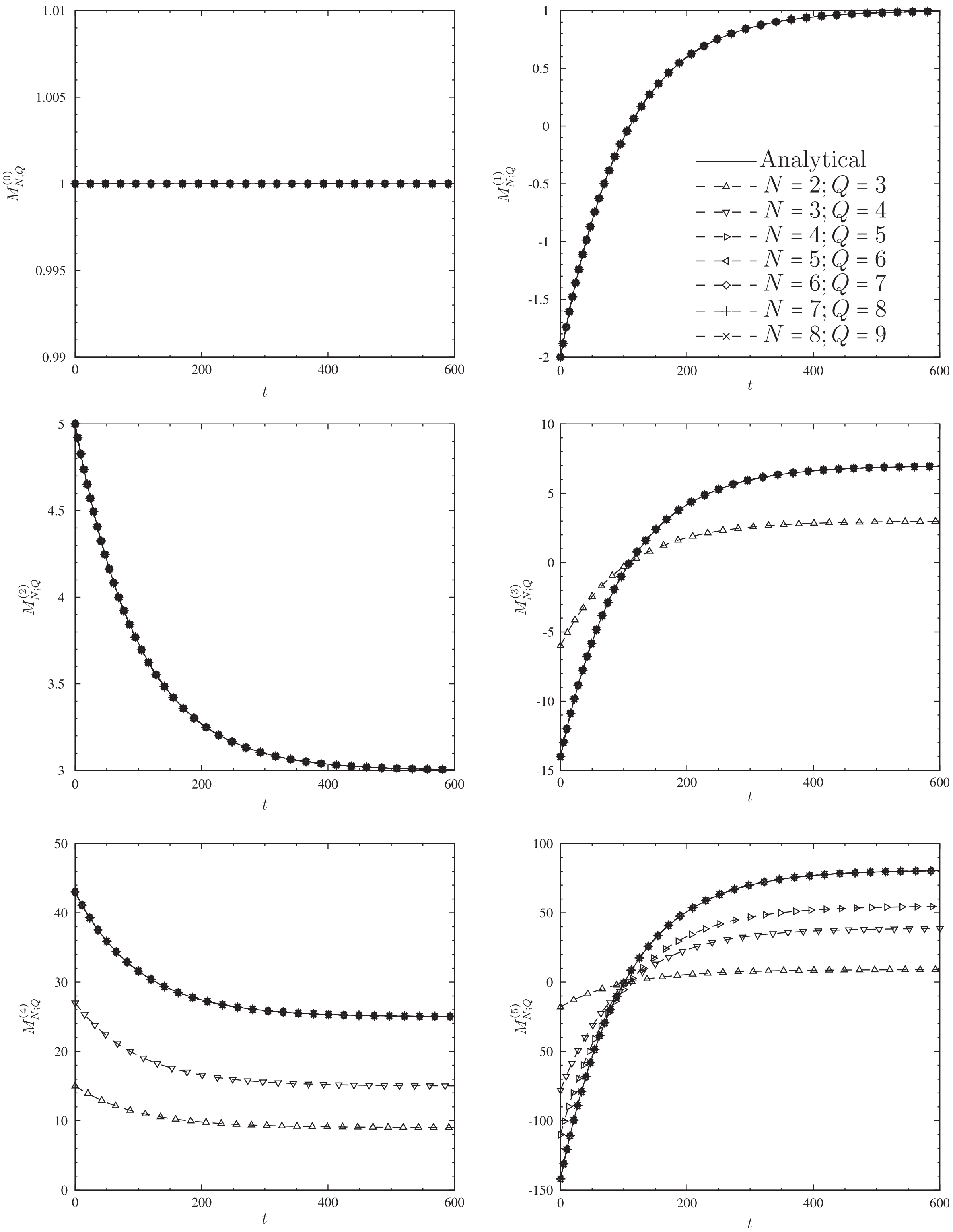

Fig. 3. Homogeneous relaxation: comparison between the evolution of the moments $\mathcal{M}^{(M)}_{N;Q}, M = 0, 1, \ldots 8$, recovered using the models GHLBM$(N; Q = N + 1), N = 2, 3 \ldots 8$, and the corresponding analytical solutions given by Eq. (27), for $n_p = 1.0, U_{p,0} = -2.0, T_{p,0} = 1.0, U_{p,*} = 1.0$ and $T_{p,*} = 2.0$.

Hermite transform remains close to a physically meaningful shape at all the times. But this does not affect the ability to recover the right values of the momenta. Of course, this is strictly true only for this simple academic case, and once again the transport will turn everything.

The advection term

Exact reasonings such as those of the preceding section cannot be extended as soon as the advection term is non null. We already mentioned that Eq. (20) was justified by projecting each term of

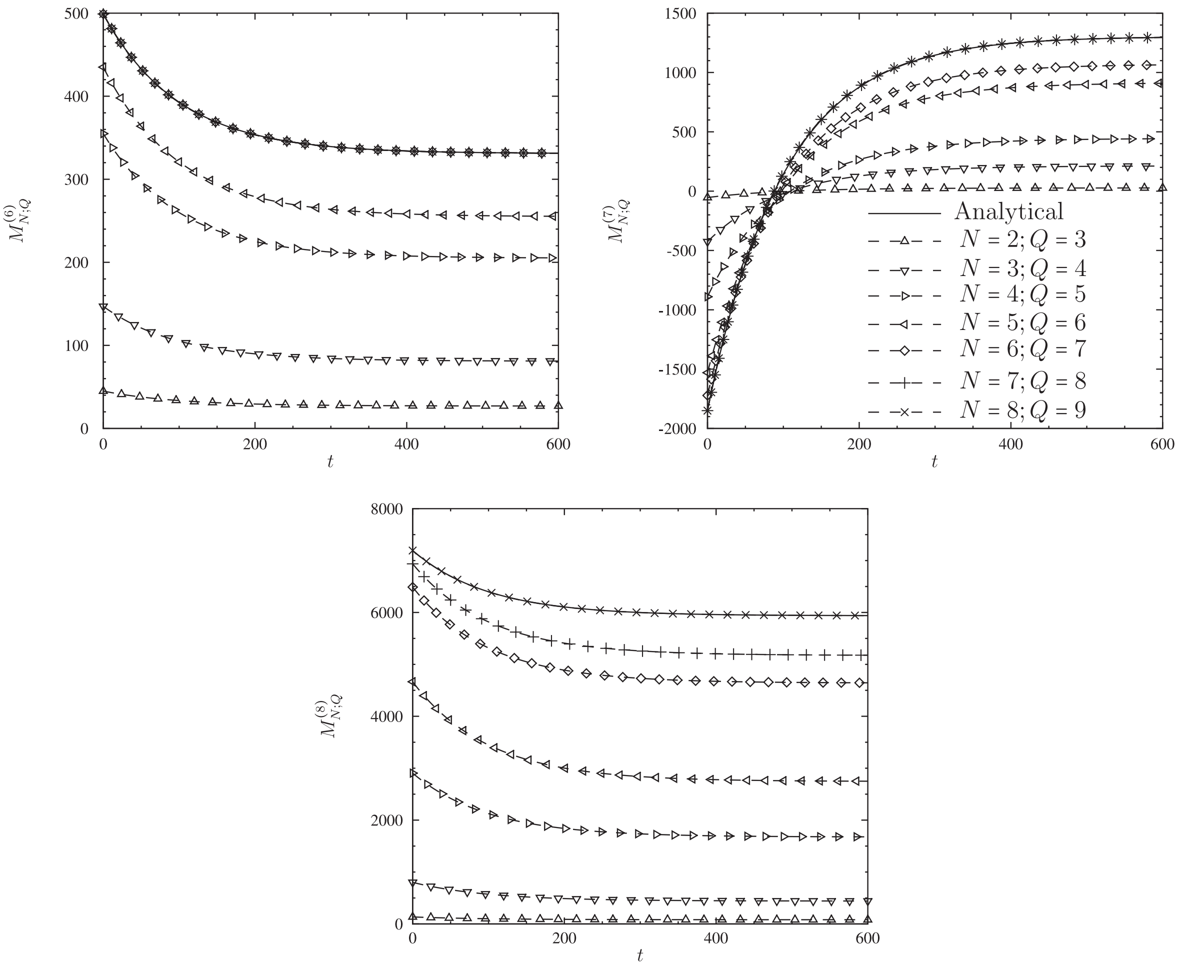

Fig. 3 (*continued*)

Eq. (12) into the space of Hermitian polynomials and truncating at order N, but that this was not rigorous for the advection term. And indeed,

$$\left(\frac{\partial f_p}{\partial t}\right)^{(N)} = \frac{\partial f_p^{(N)}}{\partial t} \tag{32}$$

$$\left(c_p\frac{\partial f_p}{\partial x}\right)^{(N)} \neq c_p\frac{\partial f_p^{(N)}}{\partial x} \tag{33}$$

$$\left(\left[\frac{U_p-(U_f+V_d)}{\tau_p}\right]\frac{\partial f_p}{\partial c_p}\right)^{(N)} = -\mathbf{A}\omega(c_p)\sum_{n=0}^{N-1}\frac{1}{n!}a_n(x,t)\mathcal{H}_{n+1}(c_p) \tag{34}$$

$$\left(\frac{2}{\tau_p}\left[f_p-f^*\right]\right)^{(N)} = \frac{2}{\tau_p}\left[f_p^{(N)}-f^{*(N)}\right] \tag{35}$$

If we define ϵ as

$$\epsilon = c_p\frac{\partial f_p^{(N)}}{\partial x} - \left(c_p\frac{\partial f_p}{\partial x}\right)^{(N)} \tag{36}$$

then $f_p^{(N)}$ satisfies the following equation,

$$\partial_t f_p^{(N)} + c_p\partial_x f_p^{(N)} - \mathbf{A}\omega(c_p)\sum_{n=0}^{N-1}\frac{1}{n!}a_n(x,t)\mathcal{H}_{n+1}(c_p) + \frac{2}{\tau_p}\left[f_p^{(N)}-f^{*(N)}\right] = \epsilon \tag{37}$$

that only departs from Eq. (20) because of ϵ at the right hand side. Using Eq. (14) and the recurrence relation $c_p\mathcal{H}_n(c_p)=\mathcal{H}_{n+1}(c_p)+n\mathcal{H}_{n-1}(c_p)$ satisfied by the Hermite polynomials (Shan et al., 2006), ϵ reads

$$\epsilon(x,t;c_p) = \partial_x\left[\omega(c_p)\sum_{n=0}^{N}\frac{1}{n!}a_n(x,t)\{\mathcal{H}_{n+1}(c_p)+n\mathcal{H}_{n-1}(c_p)\}\right] \tag{38}$$

$$-\left(\partial_x\left[\omega(c_p)\sum_{n=0}^{+\infty}\frac{1}{n!}a_n(x,t)\{\mathcal{H}_{n+1}(c_p)+n\mathcal{H}_{n-1}(c_p)\}\right]\right)^{(N)} \tag{39}$$

$$=(1/N!)\omega(c_p)\partial_x\left[a_N(x,t)\mathcal{H}_{N+1}(c_p)-a_{N+1}(x,t)\mathcal{H}_N(c_p)\right] \tag{40}$$

If this error term were null, Eqs. (20) and (37) would be identical and $\tilde{f}_p$ would match $f_p^{(N)}$ exactly. Remembering that we only need to evaluate $f_p^{(N)}$ at the quadrature points $c_{p,k}$, we would only need that $\epsilon(x,t;c_{p,k})$ be null for all $k=1,\ldots,Q$. We can turn one part of the ϵ expression to zero by noting that $Q=N+1$ ensures $\mathcal{H}_{N+1}(c_{p,k})=0$ for all $k=1,\ldots,Q$. But we then still get

$$\epsilon(x,t;c_{p,k}) = -(1/N!)\omega(c_p)\partial_x a_{N+1}(x,t)\mathcal{H}_N(c_{p,k}) \tag{41}$$

and $a_{N+1}(x,t)$ cannot be evaluated using $f_p^{(N)}$ only. Choosing to retain Eq. (20) in place of Eq. (37) is therefore equivalent to the assumption that $a_{N+1}(x,t)\simeq 0$, or more precisely that $\partial_x a_{N+1}(x,t)\simeq 0$, which is exactly the closure assumption made by Grad in his original work (Grad, 1949).

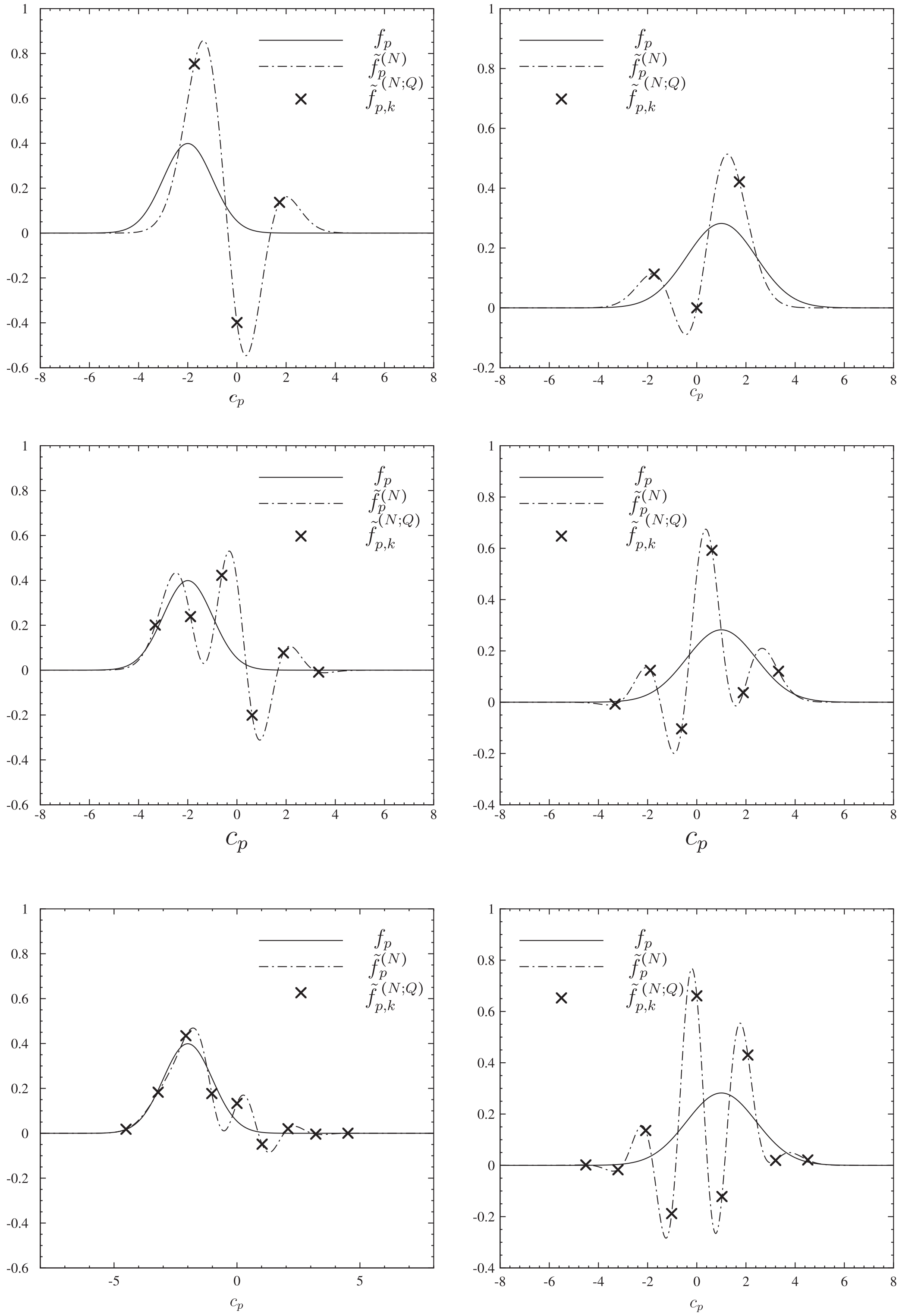

Fig. 4. Dependence of f_0 (left column) and f^* (right column) with respect to both the velocity c_p in the continuum space and the discrete velocities $c_{p,k}, k = 1, 2, \ldots Q$ with parameters $n_p = 1.0, U_{p,0} = -2.0, T_0 = 1.0, U_{p,*} = 1.0$ and $T_{p,*} = 2.0$. Solid line: analytical expressions Eq. (28); dashed-dot line: corresponding Hermite expansions, Eq. (16), for $N \in \{2, 5, 8\}$; and symbols: the corresponding values $\tilde{f}_{p,k}^{(N;Q)}$, Eq. (19) in the GHLBM($N; Q = N + 1$) model.

Deposition of inertial particles transported by a homogeneous isotropic turbulent flow

Configuration overview

Nagy and Swailes (1996) performed stochastic Lagrangian simulation for investigating the deposition of inertial particles transported by a homogeneous isotropic turbulence. The numerical domain is shown in Fig. 5. The wall is located at $x = 0$ and the top of the domain is at x_H. The particles enter at the top of the domain according to an half-Gaussian distribution of the velocity:

$$f_p(x = x_H, t; c_p < 0) = \frac{1}{\sqrt{2\pi\left\langle u'_{f@p} u'_p \right\rangle}} \exp\left[-\frac{c_p^2}{2\left\langle u'_{f@p} u'_p \right\rangle}\right]. \tag{42}$$

For particles crossing the edge, the top of the domain is a free outlet. At the wall, namely for $x = 0$, there is a perfectly absorbing boundary. Then, the PDF of particles leaving the wall is

$$f_p(x = 0, t; c_p > 0) = 0. \tag{43}$$

In random walk simulations, the particles are injected at various distances from the wall. The distance of the upper boundary of the domain is expressed as $x_H = N_L \cdot L$ where N_L is the number of particle mean free paths and L is the particle mean free path given by $L = \tau_p^t \sqrt{\left\langle u'_p u'_p \right\rangle}$. The Lagrangian particle integral time scale, τ_p^t, writes $\tau_p^t = \tau_{f@p}^t + \tau_p$ and thus the particle mean free path is

$$L = \tau_{f@p}^t \sqrt{\left\langle u'_p u'_p \right\rangle}\left(1 + \frac{\tau_p}{\tau_{f@p}^t}\right). \tag{44}$$

Nagy and Swailes (1996) considered particles with a Stokes number equal to 100. The other fluid and particles properties are then deduced from τ_p and $\tau_{f@p}^t$:

$$\tau_p = 1$$
$$\tau_{f@p}^t = 0.01$$
$$St = \frac{\tau_p}{\tau_{f@p}^t} = 100$$
$$U_f = 0$$
$$\left\langle u'_{f@p} u'_{f@p} \right\rangle = 101$$
$$\left\langle u'_{f@p} u'_p \right\rangle = 1$$
$$L = 1$$

The analysis can be either done in terms of particle mean free paths N_L or in terms of Stokes numbers. A large N_L corresponds to a small Stokes number and a small N_L corresponds to a large Stokes number.

The computations shown in the present section have been performed with $Q = 20$ discrete velocities and the order of the truncation is $N = 6$. The domain is meshed in the x-direction with an uniform mesh having $N_x = 100$ points. A flux limiter scheme (Cristea and Sofonea, 2004; Sofonea et al., 2004; Sofonea and Sekerka, 2005; Ambruş and Sofonea, 2012) was used to solve the evolution equation for $\tilde{f}_{p;k}^{(N;Q)}$ at each quadrature point $c_{p;k}$ $(1 \leqslant k \leqslant Q)$.

In the present case, after a transient phase the system reaches a steady state where the number of particles in the domain is fluctuating around a constant mean value. Then the number of injected particles are balanced with the number of deposited particles and the number of particles leaving the domain by the free outlet at the top of the domain (see Nagy and Swailes (1996) for more details).

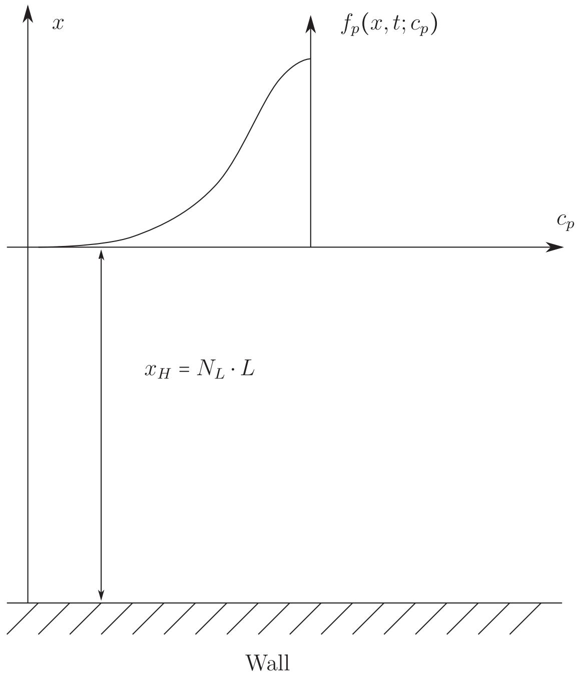

Fig. 5. Sketch of the numerical domain and the boundary condition on the PDF. At the top of the domain ($x = x_H$) a Maxwellian distribution is prescribed for $c_p < 0$ (see Eq. (42)) and at the wall a pure absorbing wall boundary condition is imposed.

Results and discussion

The dependence of the particle number density, defined by Eq. (1), on the number of mean free path and the distance to the wall is shown in Fig. 6. For heavy particles, corresponding to $N_L = 0.5$, the profile of particle number density is almost flat, meaning that the number density of particles at the wall is nearly the same as the one at the top of the domain. Indeed, such very inertial particles weakly interact with the turbulence and cross the domain up to the wall. In contrast, Fig. 6 shows that the number density of particles with a small Stokes number, corresponding to large N_L, is small at the wall. This trend was expected because in such a case the particle-turbulence interaction lead a part of the particles to go towards the wall and another part back in the flow, i.e. by the free outlet at the top boundary.

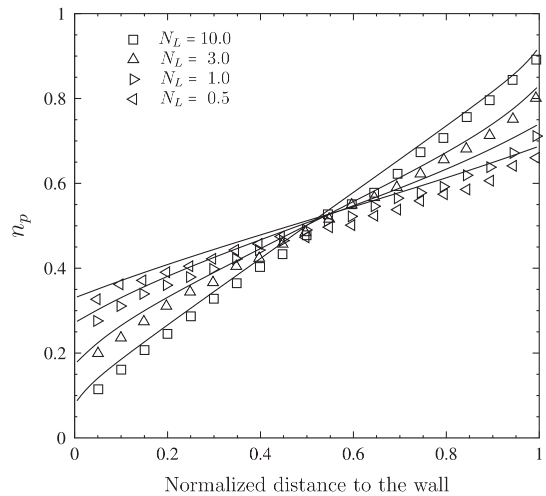

Fig. 6. Particle number density with respect to the normalised distance to the wall. The symbols are the data from Nagy and Swailes (1996) and the solid lines represent the predictions of the GHLBM.

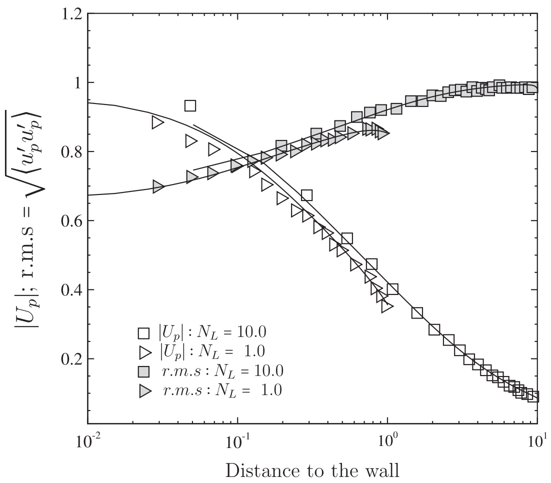

Fig. 7. Mean particle vertical velocity with respect to the distance to the wall. The symbols are the data from Nagy and Swailes (1996) and the solid lines the predictions of the GHLBM.

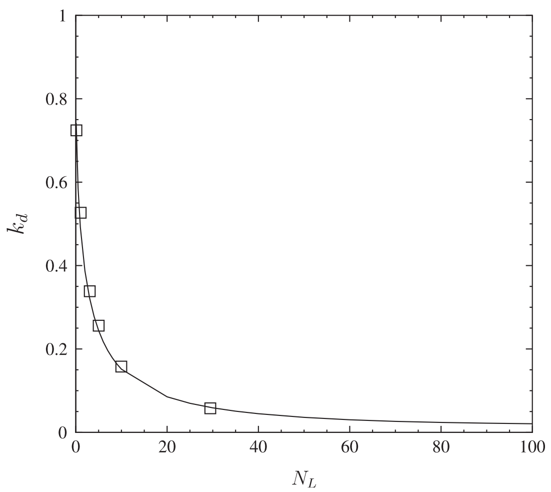

Fig. 8. Particle deposition rate with respect to the number of mean free path. The symbols are the data from Nagy and Swailes (1996) and the solid line the predictions of the GHLBM.

Fig. 6 shows that GHLBM model is in good agreement with the random walk stochastic simulation performed by Nagy and Swailes (1996). Compared to Diounou et al. (2011) the results are improved in the near wall region by use of the Hermite polynomial expansion.

Fig. 7 shows the mean vertical particle velocity and r.m.s velocity for $N_L = 10.0$ and $N_L = 1.0$. One can observe that the magnitude of the particle velocity is increasing while approaching the wall. At the opposite side, the particle r.m.s velocity is decreasing when approaching the bottom boundary condition.

Fig. 8 shows the deposition rate with respect to the number of particle mean free paths. The deposition rate, defined as

$$k_d = \frac{\int_{-\infty}^{0} c_p f_p(x = 0, t; c_p) dc_p}{\frac{1}{x_h} \int_0^{x_h} \left[\int_{-\infty}^{+\infty} f_p(x, t; c_p) dc_p \right] dx} \tag{45}$$

is the flux of particles towards the wall normalised by the bulk particle number density. A small number of particle mean free paths, i.e. $N_L \to 0$, corresponds to particles with a large inertia. Such kind of particles cross the domain without interacting with the turbulence. Thus the expected deposition rate, and the one shown by Fig. 8, is 1. In others word all particles entering in the domain at x_h are found at the wall at $y = 0$. On the other hand, particles having a large number of mean free path ($N_L \to +\infty$) have a strong interaction with the turbulence. A part of the particles deposit but also a part go back to the mean flow by the outlet at the top of the domain. As a consequence, increasing the number N_L of particle mean free paths leads to decreasing the deposition rate (as shown by Fig. 8). It is remarkable that the deposition rate predicted by the Lattice Boltzmann method is in very good accordance with the random walk Lagrangian simulations of Nagy and Swailes (1996).

Conclusions and prospects

A novel Gauss-Hermite Lattice Boltzmann Model for solving the kinetic equation describing the dynamical behaviour of solid inertial particles interacting with a turbulent flow has been proposed. For the sake of clarity the model has been developed for 1D in space and in velocity. However the extension to 3D in space and in velocity is straightforward.

A simple case of a homogeneous relaxation towards an equilibrium has been used to show the effect of the order N of the Lattice Boltzmann model. This case allowed us to show that, when a Lattice Boltzmann scheme is used, we do not solve directly for the PDF but for a projection of the true PDF on a Hermite basis. Moreover the projected PDF may have negative values, which is not possible for the true PDF. Accordingly, the boundary conditions have to be also projected on a Hermite basis.

The Lattice Boltzmann scheme has been validated for the case of the deposition of inertial particles transported by a homogeneous isotropic turbulent flow as studied by Nagy and Swailes (1996) with random walk simulations. The mean particle velocity, the particle fluctuating velocity and the deposition rate are all very well predicted by the proposed Lattice Boltzmann model. The results are in good accordance even for particles having a very small relaxation time. Such a case was the more critical because the particle kinetic energy varies strongly between the top of the domain and the wall.

By using the proposed Lattice Boltzmann scheme it is possible to implement different boundary conditions describing more complex phenomena as the bouncing of solid particles on a rough wall (Konan et al., 2009). As discussed in the introduction, the derivation of practical general wall boundary conditions in the frame of the Eulerian moment approach is a very difficult challenge and a very promising approach should be to couple the moment equations with a full resolution of the PDF transport equation in the near-wall region. Such a hybrid method has already been developed using a Lagrangian stochastic approach to solve the PDF kinetic equation (Pialat et al., 2007a; Pialat et al., 2007b), but the coupling of the Eulerian moment approach with the Lattice Boltzmann approach seems to be much more feasible. The present paper shows that this coupling can now be considered for the prediction of particle-laden turbulent flow with deposition at the wall.

Acknowledgments

This work was supported by the ANR DEPART project, Grant ANR-12-IS04-0003-01 of the French Agence Nationale de la Recherche and the grant of the Romanian National Authority for Scientific Research CNCS – UEFISCDI, Project Number PN-II-ID-JRP-2011-2-0060.

References

Abe, T., 1997. Derivation oh the lattice Boltzmann method by means of the discrete ordinate method for the Boltzmann equation. J. Comput. Phys. 131, 241–246.

Aguinaga, S., Simonin, O., Borée, J., Herbert, V., 2009. A simplified particle-turbulence interaction PDF model: application to deposition modelling in turbulent boundary layer. In: Proceedings of the ASME 2009 Fluids Engineering Division Summer Meeting, August 2–6, 2009, Vail, Colorado, USA.
Aidun, C.K., Clausen, J.R., 2010. Lattice-Boltzmann method for complex flows. Annu. Rev. Fluid Mech. 42, 439–472.
Ambruş, V.E., Sofonea, V., 2012. High-order thermal lattice Boltzmann models derived by means of Gauss quadrature in the spherical coordinate system. Phys. Rev. E 86, 016708.
Bhatnagar, P.L., Gross, E.P., Krook, M., 1954. A model for collision process in gases. i.small amplitude processes in charged and neutral one-component systems. Phys. Rev. 94, 511.
Cate, A., Derksen, J., Portela, L., Akker, H.V.D., 2004. Fully resolved simulations of colliding monodisperse spheres in forced isotropic turbulence. J. Fluid Mech. 519, 233–271.
Chen, H., Orszag, S., Staroselsky, I., 2007. Macroscopic description of arbitrary Knudsen number flow using Boltzmann-BGK kinetic theory. J. Fluid Mech. 574, 495.
Cho, H., Venturi, D., Karniadakis, G.E., 2014. Statistical analysis and simulation of random shocks in stochastic Burgers equation. Proc. Roy. Soc. Lond. A: Math. Phys. Eng. Sci. 470.
Colosqui, C., Chen, H., Shan, X., Staroselsky, I., Yakhot, V., 2009. Propagating high-frequency shear waves in simple fluids. Phys. Fluids 21, 013105.
Colosqui, C.E., 2010. High-order hydrodynamics via lattice Boltzmann methods. Phys. Rev. E 81, 026702.
Cristea, A., Sofonea, V., 2004. Two component lattice Boltzmann model with flux limiters. Central Eur. J. Phys. 2, 382–396.
Derevich, I., Zaichik, L., 1988. Precipitation of particles from a turbulent flow. Izvetiyia Akademii Nauk SSSR Mekhanika Zhidkosti i Gaza 5, 96–104.
Derksen, J.J., Sundaresan, S., 2007. Direct numerical simulations of dense suspensions: wave instabilities in liquid-fluidized beds. J. Fluid Mech. 587, 303–336.
Diounou, E., Fede, P., Fournier, R., Blanco, S., Simonin, O., 2011. Kinetic approach for solid inertial particle deposition in turbulent near-wall region flow lattice Boltzmann based numerical resolution. In: Proceedings of AJK2011-FED, ASME-JSME-KSME Joint Fluids Engineering Conference 2011, July 24–29, 2011, Hamamatsu, Shizuoka, Japan.
Friedlander, S., Johnstone, H., 1957. Deposition of suspended particles from turbulent gas stream. J. Indust. Eng. Chem. 49, 1159.
Gatignol, R., 1983. The Faxen formulae for a rigid particle in an unsteady non uniform stokes flow. J. Méc. Théor. Appl. 9, 143–160.
Grad, H., 1949. On the kinetic theory of rarefied gases. Commun. Pure Appl. Math. 2, 331–407.
Grad, H., 1952. Statistical mechanics, thermodynamics, and fluid dynamics of systems with an arbitrary number of integrals. Commun. Pure Appl. Math. 5, 455–494.
He, X., Luo, L.-S., 1997. Theory of the lattice Boltzmann method: from the Boltzmann equation to the lattice Boltzmann equation. Phys. Rev. E 56, 6811–6817.
Hinze, J., 1972. Turbulent fluid and particle interaction. Prog. Heat Mass Transfer 6, 433–452.
Kallio, G.A., Reeks, M.W., 1989. A numerical simulation of particle deposition in turbulent boundary layers. Int. J. Multiphase Flow 15, 433–446.
Konan, N., Kannengieser, O., Simonin, O., 2009. Stochastic modeling of the multiple rebound effects for particle-rough wall collisions. Int. J. Multiphase Flow 35, 933–945.
Laviéville, J., Deutsch, E., Simonin, O., 1995. Large eddy simulation of interaction between colliding particles and a homogeneous isotropic turbulence field. 6th Int. Symp. On Gas-Solid Flows, vol. 228. ASME FED, pp. 347–357.
Liu, B.Y., Agarwal, J.K., 1974. Experimental observation of aerosol deposition in turbulent flow. J. Aerosol Sci. 5, 144–155.
Marchioli, C., Picciotto, M., Soldati, A., 2007. Influence of gravity and lift on particle velocity statistics and transfer rates in turbulent vertical channel flow. Int. J. Multiphase Flow 33, 227–251.
Matida, E., Nishino, K., Torii, K., 2000. Statistical simulation of particles deposition on the wall from turbulent dispersed pipe flow. Int. J. Heat Fluid Flow 21, 389–402.
Maxey, M., Riley, J., 1983. Equation of motion for a small rigid sphere in a non uniform flow. Phys. Fluids 26, 2883–2889.
Nagy, T.K., Swailes, D., 1996. Random walk approach for simulation of particle deposition from turbulent flows. Periodica Polytech. Ser. Mech. Eng. 40, 143–156.
Pialat, X., Simonin, O., Villedieu, P., 2007a. A hybrid Eulerian-Lagrangian method applied to turbulent gas-solid channel flow. In: 6th International Conference on Multiphase Flow, ICMF 2007, Leipzig, Germany.
Pialat, X., Simonin, O., Villedieu, P., 2007b. A hybrid Eulerian-Lagrangian method to simulate the dispersed phase in turbulent gas-particle flows. Int. J. Multiphase Flow 33, 766–788.
Piaud, B., Blanco, S., Fournier, R., Ambruş, V.E., Sofonea, V., 2014. Gauss quadratures – the keystone of lattice Boltzmann models. Int. J. Modern Phys. C 25, 1340016.
Piaud, B., Blanco, S., Fournier, R., Clifton, M.J., 2005. Energy-conserving lattice Boltzmann thermal model in two dimensions. J. Stat. Phys. 121, 119.
Reeks, M.W., 1992. On the continuum equations for dispersed particles in nonuniform flows. Phys. Fluids 4, 1290–1303.
Reeks, M.W., 1993. On the constitutive relations for dispersed particles in nonuniform flows. I: Dispersion in a simple shear flow. Phys. Fluids 5, 750–761.
Shan, X., He, X., 1998. Discretization of the velocity space in the solution of the Boltzmann equation. Phys. Rev. Lett. 80, 65–68.
Shan, X., Yuan, X., Chen, H., 2006. Kinetic theory of hydrodynamics: a way beyond the Navier–Stokes equations. J. Fluid Mech. 550, 413–441.
Shizgal, B., 2015. Spectral Methods in Chemistry and Physics. Springer.
Simonin, O., 2000. Statistical and continuum modelling of turbulent reactive particulate flows. Part 1: Theoretical derivation of dispersed eulerian modelling from probability density function kinetic equation. In: Lecture Series 2000-06, Von Karman Institute for Fluid Dynamics, Rhodes Saint Genèse (Belgium). Von Karman Institute for Fluid Dynamics.
Simonin, O., Deutsch, E., Minier, J., 1993. Eulerian prediction of the fluid/particle correlated motion in turbulent two-phase flows. Appl. Sci. Res. 51, 275–283.
Sofonea, V., Lamura, A., Gonnella, G., Cristea, A., 2004. Finite-difference lattice Boltzmann model with flux limiters for liquid–vapor systems. Phys. Rev. E 70, 046702.
Sofonea, V., Sekerka, R.F., 2005. Diffuse-reflection boundary conditions for a thermal lattice Boltzmann model in two dimensions: evidence of temperature jump and slip velocity in microchannels. Phys. Rev. E 71, 066709.
Succi, S., 2001. The Lattice Boltzmann Equation for Fluid Dynamics and Beyond. Clarendon Press, Oxford.
Tchen, C., 1947. Mean value and correlation problems connected with the motion of small particles suspended in a turbulent fluid. Ph.D. thesis, Delft, Martinus Nijhoff, The Hague.
Van Dijk, P., Swailes, D., 2012. Hermite-DG methods for PDF equations modelling particle transport and deposition in turbulent boundary layers. J. Comput. Phys. 231, 4904–4920.
Xiu, D., Karniadakis, G.E., 2002. The Wiener–Askey polynomial chaos for stochastic differential equations. SIAM J. Sci. Comput. 24, 619–644.
Young, J., Leeming, A., 1997. A theory of particle deposition in turbulent pipe flow. J. Fluid Mech. 340, 129–159.
Zaichik, L., Pershukov, V., Kozelev, M., Vinberg, A., 1997. Modeling of dynamics, heat transfer, and combustion in two-phase turbulent flows: 1. Isothermal flows. Exp. Thermal Fluid Sci. 15, 291–310.
Zhang, R., Shan, X., Chen, H., 2006. Efficient kinetic method for fluid simulation beyond the Navier-Stokes equation. Phys. Rev. E 74, 046703.